Testing the Silica Leakage Hypothesis

Lauren McLean

Submitted in partial fulfillment of the requirements for the degree of Combined Honours Bachelor of Science in Earth Sciences and Oceanography

at

Dalhousie University
Halifax, Nova Scotia
April, 2008

Table of Contents

Figures

Tables

Abstract

The silica leakage hypothesis is one mechanism put forth to explain lower atmospheric CO_2 levels during glacial times. Measuring the percent opal from sediment cores recovered in the Eastern and Western Equatorial Pacific (EEP and WEP) and plotting it against time tests the validity of the opal leakage hypothesis. During glacial times a build up of silicic acid occurs in the Southern Ocean (SO) due to low diatom productivity. The excess silicic acid is transported to low latitude waters in the Pacific Ocean via Antarctic Intermediate Water. The silica rich water is upwelled at the Equator where the silicic acid is taken up by diatoms. The opaline frustules become incorporated into the sedimentary record when the diatom dies. The percent opal of sediment samples can be determined from recovered cores. Cores TR163-22 and ME 24 from the EEP show a strong increase in the percent opal 40-60 ka however the cores from the WEP, MD98-2181 and MD06-3067 do not have this signal. There is no increase in any core during the Last Glacial Maximum (LGM). Therefore contribution by the silica leakage hypothesis in reducing CO_2 during glacial times is believed to be small.

Keywords: silica leakage hypothesis, silicic acid, CO_2, Eastern and Western Equatorial Pacific

1.0 INTRODUCTION

Atmospheric carbon dioxide (CO_2) concentrations determined from the Vostok ice core in Antarctica show average CO_2 concentrations of 180-200 parts per million (ppm) during peak glacial times (Petit et al. 1999). Since the Last Glacial Maximum (LGM) approximately 18 ka, CO_2 levels have increased by 80-100 ppm. Prior to the industrial revolution, CO_2 concentrations were roughly 280 ppm; however, anthropogenic activities have since contributed 70-90 ppm to atmospheric CO_2 concentrations (Sigman and Boyle 2000).

CO_2 is a natural component of the Earth's atmosphere. Though a relatively small fraction of the Earth's atmosphere, it strongly influences global temperatures due to its greenhouse effect. The role of CO_2 as a greenhouse gas directly links it to past climate change and predictably future climate change.

The World Ocean is only second in the abundance of carbon to the sediment and crust of the earth. However, carbon in the deep ocean has a residence time of approximately 1000 years compared to carbon in the Earth's crust which has a residence time of 250-300 Myr (Sigman and Boyle 2000). On glacial and interglacial timescales the reservoir of carbon in the deep ocean has the ability to affect atmospheric CO_2 through partial pressure relationships with aqueous CO_2 in the ocean.

Many factors need to be considered to elucidate the reasons for the natural oscillations of atmospheric CO_2. The ocean is the only reservoir big and reactive enough to account for CO_2 oscillations on glacial/interglacial time scales (Matsumoto et al. 2002). An increase of 80-100 ppm in atmospheric CO_2 needs to be explained by one or more factors. Carbon and CO_2 storage, ocean temperature, ocean salinity and the ocean carbon cycle all influence atmospheric CO_2. The terrestrial carbon reservoir decreases during times of glaciation due to extended ice cover on land and thus the drawdown of atmospheric CO_2 diminishes. Due to buffering by the carbon reservoir in the oceans and the balance of calcium carbonate ($CaCO_3$) the addition of CO_2 from this source is minimal. As well, the carbon reservoir on land acts as a source not a sink for CO_2 during glacial periods which does not explain the decrease in CO_2. The drawdown of CO_2 into the ocean also depends on temperature and salinity; CO_2 is less soluble in warm water then cold and increased salinity reduces CO_2 solubility. During glacial times the ocean would have been colder at the surface leading to a greater CO_2 drawdown into the world ocean. Due to the large quantity of ice during glaciations the world ocean contained more salt; this reduces the solubility and increases atmospheric CO_2. The effect of the above factors on atmospheric CO_2 concentrations is minimal at best. Therefore the influence on atmospheric CO_2 attributed to the above factors is not the main reason for the 80-100 ppm increase seen between glacial and interglacial periods (Sigman and Boyle 2000). In fact, a hypothesis is needed to explain the low levels of atmospheric CO_2 on a scale that fit both the magnitude in change and the time it took for the change to occur. The opal leakage hypothesis aims to do just that.

1.1 Silicic acid in the World Ocean and sedimentary opal records

The distribution of nutrients in the world ocean differs with respect to location and depth. Silicic acid is concentrated in surface waters of the Southern Ocean (SO) that surround Antarctica, as well as in the Northern Pacific. Both areas of concentrated silicic acid are due to the upwelling of silica rich deep water. Figure 1.10 shows the distribution of silicic acid in surface waters of the world ocean and Figure 1.11 shows the distribution of silicic acid with respect to depth. During interglacial times the Southern Ocean is preferentially stripped of silicic acid by diatoms in surface waters. Glacial times observe an increase in iron availability equated with an increased dust flux to the SO. Iron availability limits the uptake of silicic acid to nitrate in diatoms (Brzezinski et al. 2002). A build up of silicic acid can also occur in the SO if the number of diatoms are reduced or displaced. Extended sea ice cover stops the production of diatoms in the area where the ice covers the water. If a different phytoplankton species out competes diatoms then a build up of silicic acid could also occur because it is not being taken up by diatoms. If the later is true there is no way to prove this as the phytoplankton, phaeocystis is not preserved in the sedimentary record (Matsumoto et al. 2002). The excess silicic acid is incorporated into Subantarctic Mode Water (SAMW) and transported to low latitude regions of the Eastern and Western Equatorial Pacific (EEP and WEP respectively). Opal records from the SO show a decrease in opal burial during glacial times and an increase during interglacial times. The EEP and upwelling regions of coastal Peru show the opposite; high burial rates of opal during glacial times and low burial rates during interglacial times (Kienast et al. 2006).

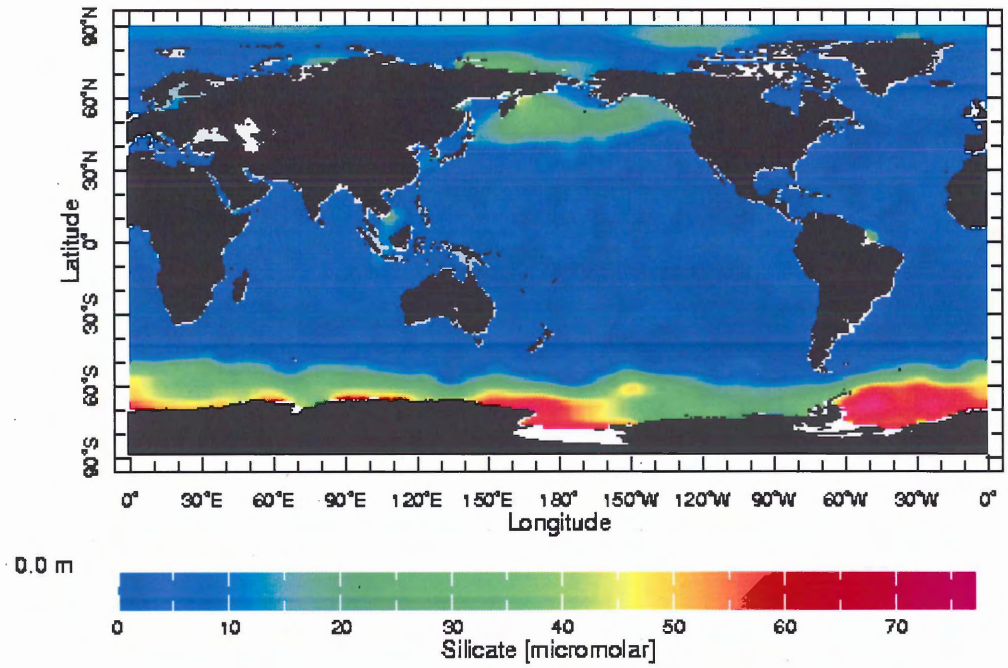

Figure 1.10 Distribution of silicate in the World's Ocean at the sea surface (http://iridl.ldeo.columbia.edu/SOURCES/.LEVITUS94/.ANNUAL/.)

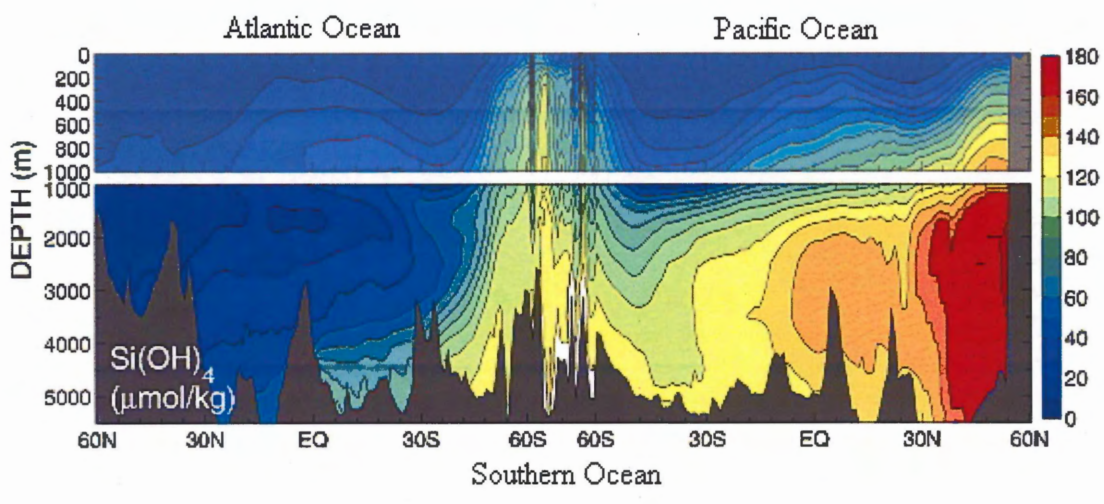

Figure 1.11 Profile of silica distribution with depth comparing the Atlantic and Pacific Oceans. 60°S is representative of the Southern Ocean. Note the maximum silicic acid concentration occurs at the surface in the Southern Ocean (Sarmiento et al. 2007).

1.2 Opal Leakage Hypothesis

The Opal Leakage Hypothesis is one of many possibilities that accounts for the difference in CO_2 levels between glacial and interglacial periods. The significant decrease during glacial times is essentially brought on by a shift in dominant organisms. Two organisms, the coccolithophorid and diatom, constitute a substantial amount of marine sediments. Coccolithophorids have calcareous shells while diatoms have siliceous. (Matsumoto et al 2002). Dust fluxes during times of glaciation bring into the oceans increased amounts of iron to the Sub-Antarctic and Antarctic regions. The iron affects the uptake ratio of silicic acid to nitrate. Typically the $Si(OH)_4:NO_3^-$ ratio in diatoms is 4:1, however; with the iron limitation in affect the ratio becomes more like 1:1; leaving the SO depleted in nitrate and oversaturated in silicic acid (Sarmiento et al 2004, Brzezinski et al. 2002). Iron deficient conditions during interglacial periods reduce nitrate uptake in diatoms; iron rich conditions during glacial periods the $Si(OH)_4:NO_3^-$ ratio lowers and SO surface waters become depleted in nitrate and oversaturated in silicic acid (Brzezinski et al. 2002). Extended sea ice cover in the Antarctic also diminishes the production of diatoms and the utilization of silicic acid (Takeda 1998). The excess silicic acid is transported via Sub-Antarctic Mode Water (SAMW) to the low latitudes of the Pacific Ocean. In regions of upwelling, mainly along the equator and off the coast of Peru, silicic acid is returned to the surface waters where it is taken up by diatoms to create their opaline structures. Usually, silicic acid is scarce in low latitude oceans and regions of upwelling (Kienast et al 2006). Glacial periods should then show an increase in the amount of biogenic opal in the sedimentary record in equatorial and upwelling regions of the Pacific Ocean.

Due to the availability of nitrate and silicate, diatoms in upwelling regions of the low latitude Pacific dominate the glacial scene. The alkalinity of sea water is balanced by the influx of sediment from continental weathering and the removal of $CaCO_3$ through burial. Alkalinity increases during glacial periods when calcareous coccolithophorids are out stripped by siliceous diatoms. This imbalance perturbs the equilibrium that exists between alkalinity and Dissolved Inorganic Carbon (DIC); Equation 1.0 expresses the equilibrium between the two. To restore equilibrium an increase in the burial of $CaCO_3$ must occur. Therefore the carbonate compensation depth increases in depth to allow more calcium carbonate to be buried. If this is the case then $CO_{2\ (aq)}$ must also be used to produce HCO_3^-. The use of oceanic CO_2 effectively draws down atmospheric CO_2 to restore balance (Bradtmiller et al. 2006).

$$CO_{2\ (aq)} + H_2O + CO_3^{2-} \leftrightarrow 2HCO_3^- \qquad (1.0)$$

1.3 Recent studies on low-latitude Pacific sedimentary opal records and modifications of the opal leakage hypothesis

Matsumoto et al. (2002) first proposed the opal leakage hypothesis. However, this thesis uses the differing results from Bradtmiller et al. 2006 paper and Kienast et al. 2006 paper as an avenue to test the silica leakage hypothesis further. Bradtmiller et al. reject the hypothesis but restricted their work to the last 30 000 years. Kienast et al. found supporting evidence and ventured back 150 000 years in the sedimentary record but used cores mostly found in the EEP.

The objective of this thesis is to expand the testing of the opal leakage hypothesis in space and time which will add to the findings of the above mentioned papers. Core locations will be taken from the WEP, EEP and upwelling regions off the coast of Peru. The time range represented in the cores ranges from 30 000 to 250 000 years.

2.0 PROCEDURE

2.1 Study Area

The study area is located in the EEP and WEP with 2 cores in each region as shown in Figure 2.1. Cores TR163-22 and ME0005A-24JC (ME 24) are situated in the EEP. Core TR163-22 is located at 0.1°N, 86.3°W at a depth of 2941 m. Core ME 24 is located at 0.31°N, 92.24°W at a depth of 2830 m. Cores MD06-3067 and MD98-2181 are located in the WEP. Core MD06-3067 is located at 6.3°N, 126.3E at a depth of 1574 m and core MD98-2181 is located at 6.3°N, 125.83°E at a depth of 2114 m.

2.2 Wet Chemistry

The following procedure outlines the steps for determining the biogenic opal in pelagic sediment modeled after Mortlock and Froelich's 1989 paper. Some steps were altered in order to accommodate the smaller sample size of 20 mg versus 25-200mg. A smaller sample size is used to conserve the sediment for other tests. All lab ware is plastic not glass (silica) in order to reduce the potential error incurred from glassware. The procedure is broken up into 4 days.

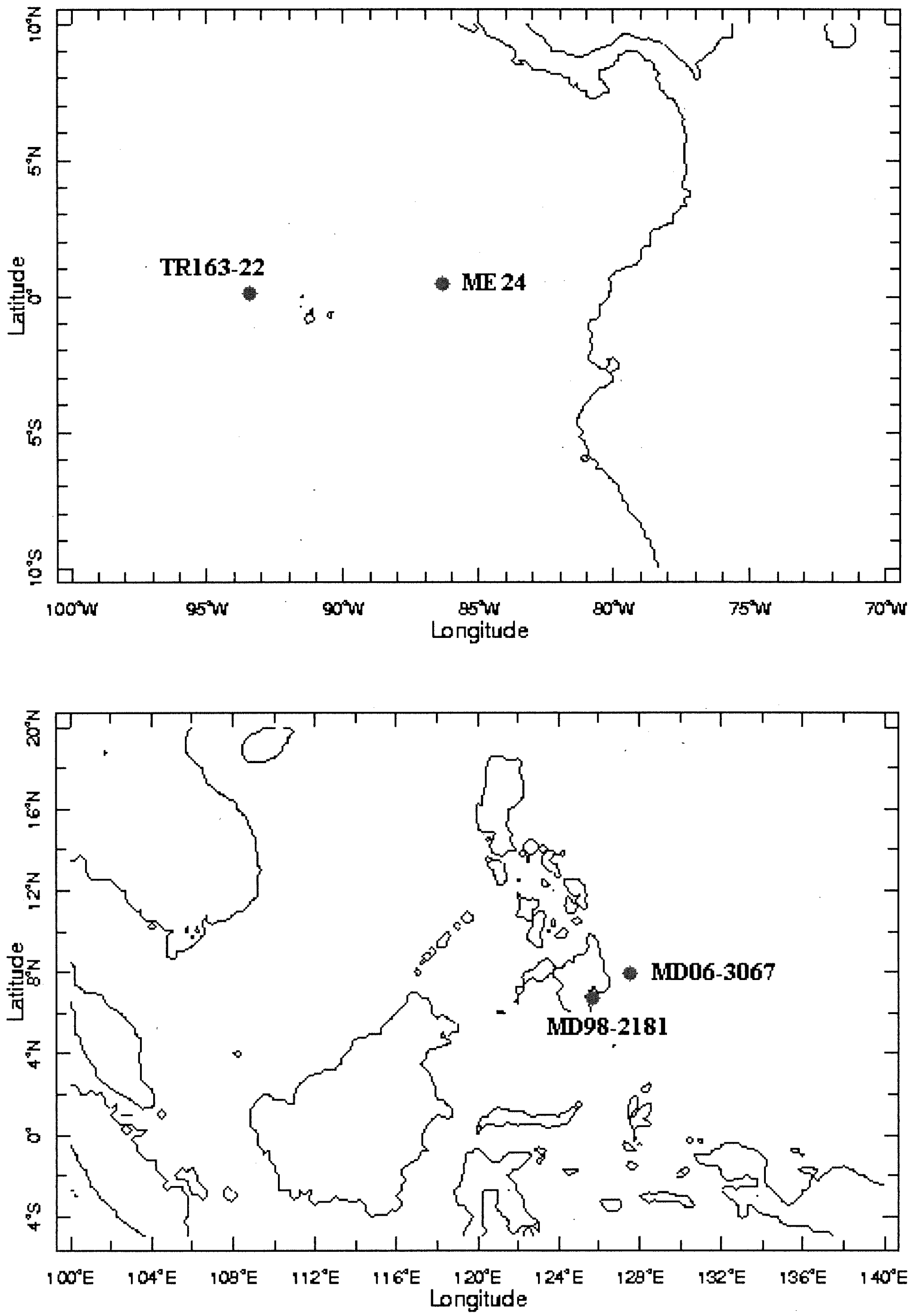

Figure 2.1: Locations of the 4 cores used for analysis. The top map is located in the Western Equatorial Pacific and the bottom map is off the coast of South America in the Eastern Equatorial Pacific. (http://iridl.ldeo.columbia.edu/SOURCES/.LEVITUS94/.ANNUAL/.temp/)

On day one, the ground sediment samples were weighed, approximately 20mg, and placed into centrifuge tubes. A batch of 96 sediment samples is possible which included calibration standards, internal standards and blanks.

On day two each tube received 2 millilitres (ml) of 10% H_2O_2 and then was immediately swirled. The H_2O_2 was added in order to oxidize the organic matter. After a ½ hour wait, 2ml of 10% HCl were added to each tube in order to dissolve the inorganics present ($CaCO_3$). Next, in batches of 32, the tubes were sonicated for a ½ hour which breaks up cell membranes. After sonication, 20ml of Doubly Deionized Water (DDW) were added to each tube using an Eppendorf repipetor. While dispensing the DDW the sides of the tube were washed down. The tubes were then centrifuged for 10 minutes at 4000 revolutions per minute (rpm) and the supernatant was decanted. All tubes were placed in an oven at 50°C and dried overnight.

On day three a water bath was prepared at 85°C. Before placing the tubes in the water bath, 20 ml of 2M Na_2CO_3 were dispensed into each tube. After 1.5 hours in the bath each tube was vortexed. One hour later, each tube was swirled, and swirled again one hour later. The tubes were left in the bath for 1.5 hours without disturbing the sediment. Redox bottles (30 ml nalgene bottles) were labelled the same as the centrifuge tubes before dispensing 10 ml of DDW into each bottle with a repipetor. After a total of 5 hours in the bath, 100 μl from each centrifuge tube were placed in its corresponding redox bottle. At this time a set of calibration standards of known silica concentration also have 100 μl extracted and dispensed in a corresponding redox bottle. An oxidant and reductant were prepared. The oxidant was a 1:1 volumetric ratio of ammonium molybdate and hydrochloric acid (HCl). The reductant was a 1:1:1 volumetric ratio of metol-sulphite, oxalic acid and sulphuric acid. 4ml of oxidant were added to each redox bottle at 10 second intervals. The same was done with the reductant in the amount of 6 ml, 20 minutes after the oxidant was added. Caps were then placed onto the redox bottles which were placed in a dark area overnight to allow the samples to colour.

On the fourth and final day the samples were read in the spectrophotometer at 812 nm. The spectrophotometer is first 'zeroed' using DDW meaning all sample values are relative to the DDW. A light is shone through the sample at a wavelength of 812 nm; the relative absorbance of the wavelength to the DDW is then displayed on the computer screen. The value read on the computer is the absorption value which along with the weight of sediment is used to calculate the % opal of each sediment sample (see below).

2.3 Calculations

The results for the four cores used in this thesis were obtained by taking the absorption unit recorded off the spectrophotometer and converting that into percent opal. Equation 2.3 illustrates how the absorption unit is calculated into percent opal. The absorption unit is multiplied by the inverse of the slope given by the calibration curve of known silica molarity. The weight is the sample weight of the sediment given in milligrams. The constant 2.4 is multiplied by the final result to correct for the high water content of radiolarians that are present in the sample (Mortlock and Froelich 1989).

$$((au * 1/slope) / weight * 56.172) * 2.4 = \text{percent opal} \qquad (2.3)$$

2.4 Sources of Error

To monitor and assess the error associated with the procedure blanks, calibration standards and internal standards were added to each batch of samples. The blanks presumably should have an absorption reading on the spectrophotometer close to 0.0 absorbance units (au); in the Mortlock and Froelich 1989 paper the reading for blanks was no higher then .003 au. However, the operational blanks for this thesis recorded absorption units of much higher values. The overall au average of all the blanks was .0318 which is 12 times higher than the values given by Mortlock and Froelich. The difference in values is believed to stem from the absorption of light by the chemicals used. To test this, two solutions were prepared that had not undergone the analytical process. The first solution contained DDW and the chemicals associated with the oxidant and reductant. An absorbance unit of .0105 was recorded. The second solution contained the same as the first but 100 μl of Na_2CO_3 was added. This solution gave a reading of .0285 au. Since, all the samples tested in the spectrophotometer had Na_2CO_3 added the unusually high blanks are considered normal for this procedure. Simply by subtracting the average blank au from the recorded au value for the samples solves this source of error. As well, more then the suggested 2-3 blanks were used with each batch of samples to get a collective average. In Table 2.41 the absorption units for all the blanks are given along with the overall average and standard deviation. Overall the reproducibility of the blanks was poor with a standard deviation of ±.0083, however; individual standard deviations better illustrate the reproducibility of the blanks within each analytical batch.

	Analytical Batch #	Au values for Blanks	Standard Deviation	Relative Standard Deviation (%)
	1	0.0219, 0.0205, 0.0213	0.0007	3.308
	2	0.0225, 0.0253, 0.0327, 0.0254	0.0044	16.48
	3	0.0424, 0.0378, 0.0406, 0.0446	0.0029	6.957
	4	0.0374, 0.0344, 0.0336, 0.0370	.0019	5.290
Overall Average au for Blanks		0.0318		
Overall Standard Deviation		0.0083		

Table 2.41: Demonstrates the reproducibility of the blanks within each analytical batch.

Six calibration standards in all were prepared at the beginning to allow the use of them in each batch of samples. The calibration standards are prepared by diluting the primary standard in order to get known molarities (in mM) of silica. This allows a calibration curve to be calculated; the graph allows for the calculation of the inverse of the slope. The inverse of the slope gives a value that can be compared to the values Mortlock and Froelich give as well as used in the calculation for percent opal. A sample calibration curve is given in Figure 2.41 for the first set of samples run. In Mortlock and Froelich, the inverse of the slope for any given calibration curve is 9.2 ± 0.2. Table 2.42 shows the values for the four rounds of analyses with and without the blank correction applied. Without the blank corrections the inverse of the slope on average is 8.65, however with the correction (subtracting the blank au from the sample au) the inverse of the slope has been in accordance with Mortlock and Froelich's value with an average of 9.39. As well, in each batch of samples 2 known sediment samples, JV Bulk and SN Bulk are run to ensure like values each time.

Analytical error associated with the spectrophotometer can be reduced by re-zeroing every 7-8 samples. In order to monitor the drift that occurs with the spectrophotometer samples are measured more then once during the 2-3 hour time it takes to record au values for all 90+ samples. This helps to determine if the spectrophotometer has to be re-zeroed and to see the analytical error that is produced from the spectrophotometer. Table 2.43 represents the four times JV Bulk and SN Bulk were recorded during one session with the spectrophotometer. The average relative standard deviation between the two samples is 0.47% which is negligible compared to the RSD's calculated in Table 2.42.

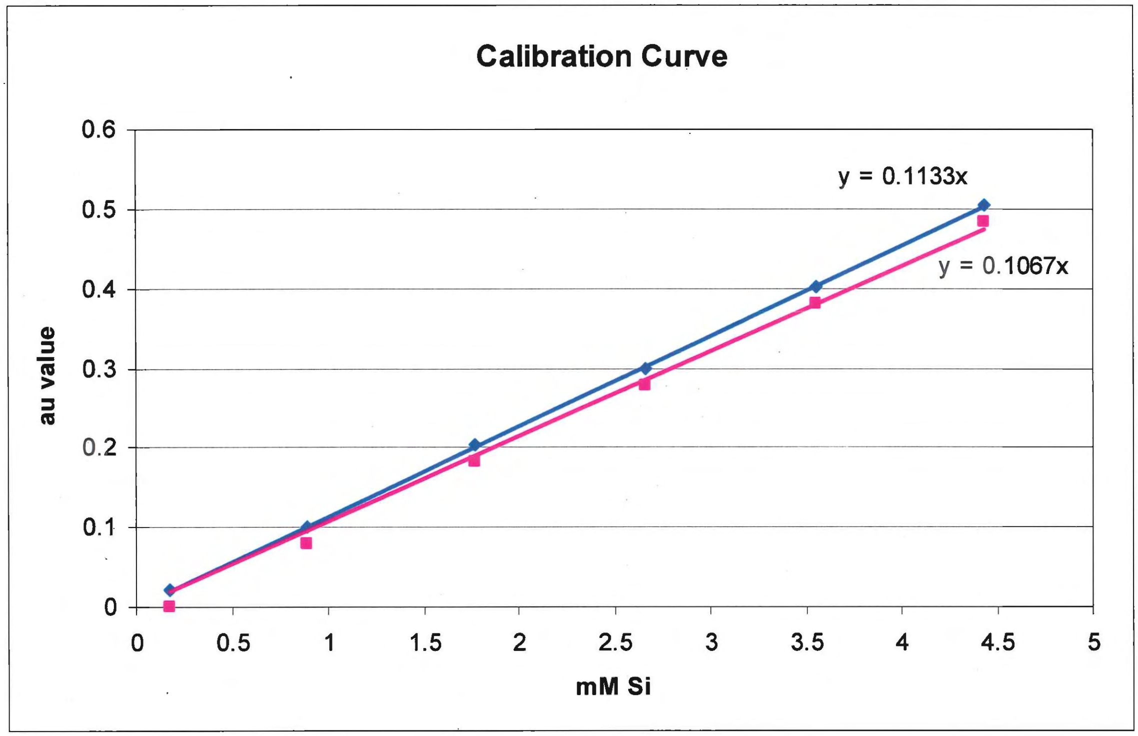

Figure 2.41: Gives the calibration curve for the first analytical batch. The pink line represents the curve without corrections to account for the high au values given by the balnks. The blue line is the corrected curve.

Batch #	1	2	3	4
1/slope	8.83	8.86	8.58	8.34
1/slope corrected	9.37	9.55	9.45	9.19

Table 2.42: Gives the values of 1/slope for the calibration curve for each analytical batch. The Mortlock and Froelich value for 1/slope is 9.2 ± 0.2 which corresponds to the corrected values (taking into account the blanks).

Sample	Absorption unit				RSD
JV Bulk	.5053	.5096	.5062	.5082	0.33%
SN Bulk	.2266	.2271	.2255	.2236	0.60%

Table 2.43: Demonstrates the little variation in absorption units as a result of analytical error produced by the spectrophotometer. RSD is the relative standard deviation.

The reproducibility of the procedure is calculated from running sediment from the same sample through multiple analytical batches. This allows for the error associated with the procedure to be assessed. Table 2.44 gives the percent opal values for the same sample run with different analytical batches. As well the standard deviation and relative standard deviation is given in order to compare the percent opals with differing magnitudes. The 6th repeat for samples 67 I 90 and 67 V 90 are ignored from the calculations as they are considered to be outliers. The RSD ranges from 4.0 to 6.4% with an average of 5.1%. This means that for any given value of percent opal a range of plus or minus 5.1% of the value is a more accurate representation of percent opal.

Sample	% Opal (repeated for same sample)						SD	RSD
67 I 90	3.7	4.4	4.2	4.1	3.8	6.5	0.26	6.4%
67 V 90	4.9	5.0	5.3	4.6	4.6	7.7	0.26	5.3%
JV Bulk	11.9	11.1	12.2				0.47	4.6%
SN Bulk	30.4	32.4	34.0				1.5	4.0%

Table 2.44 The ability to reproduce results using the same sample and the error associated with the procedure. SD is the standard deviation and RSD is the relative standard deviation.

3. RESULTS

The results are presented in two ways: one as percent opal versus depth and the other as percent opal versus age. When interpreting both sets of data analytical error, resolution of cores and location were all taken into consideration. The analytical error determined in the procedure outlined previously is ± 5.1% for any given value of percent opal. The resolution of the cores differs for each one according to how many samples were used for their given depth and age. The resolutions for each core are given in Table 3.0. A higher frequency in sampling gives a more complete depth profile and therefore is considered more accurate. However, more than those factors listed above affect the percent opal preserved in a core. The dilution of opal that occurs from the photic zone to the ocean floor, the rate of dissolution and the preservation of opal all affect the outcome of percent opal. These three factors however are not considered in the results section but are explored further in the discussion.

The main focus for the graphs was to determine periods of high percent opal versus periods of low percent opal. The transition from one to the other is not a concern. In order to tell the difference between a point and a period of high or low percent opal more than five data points need to be almost equivalent. Therefore some high and low points on the graphs are ignored as only the larger signals in percent opal are acknowledged and discussed in this thesis.

	MD06-3067	MD98-2181	TR163-22	ME 24
Resolution	1066 yrs	803 yrs	2318 yrs	1063 yrs

Table 3.0: The resolution of each core is calculated by dividing the number of samples taken per core into the time span the core represents in order to get the number of years one sample represents.

3.1 Percent Opal versus Depth

Figure 3.10 shows the distribution of percent biogenic opal for core MD06-3067 located in the WEP. The first 250 cm of the core represent a section of slightly reduced biogenic opal leading to an overall increase of 0.5 % which occurs after 250 cm to an approximate depth of 1460 cm. After 1460 cm a drop of 1.5 % is seen which then steadies at a percent opal of 3.1. From 0-250 cm the average percent opal is 4.1. Slightly higher between 250 and1460 cm is an average of 4.6%. The last 90 cm of the core drops to an average of 3.1%. The difference in percent opal for different depth ranges is very close to the analytical error of ± 5.1%. A trend is described despite this problem due to the location of the core in the open ocean of the WEP and its resolution with respect to depth. Four outliers occur on the graph at depths of 90, 120, 250 and 690 centimetres. Each sample was redone to test the validity of the suspected outliers. No specific errors were recorded for any of these samples during the first time through the procedure and therefore are included in the results, however; error may have occurred without notice.

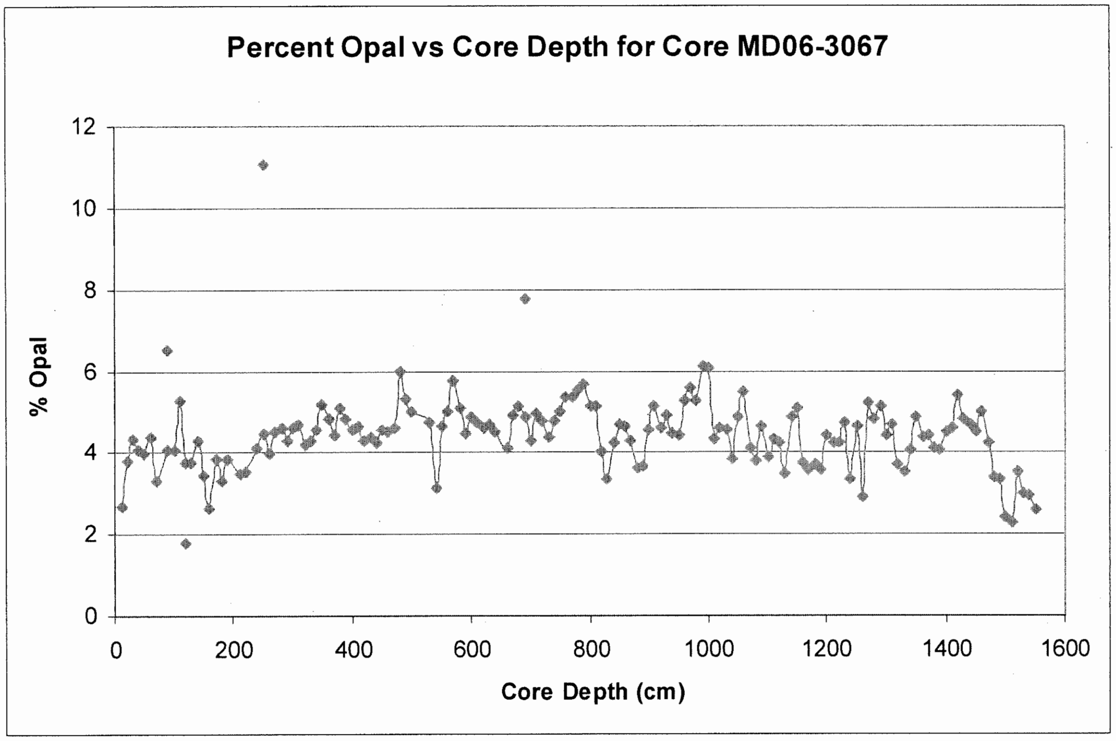

Figure 3.10 Percent opal versus the core depth for core MD06-3067.

Core MD98-2181 was taken from an embayment close to core MD06-3067 in the WEP. The graph for percent opal versus core depth for this core is seen in Figure 3.11. No distinct trends with respect to an increase or decrease in percent opal are seen in this core. Since the core was recovered from an embayment it is assumed that the fluctuation seen in the open ocean with respect to nutrients is not as apparent in enclosed areas. Therefore the trend for the graph in Figure 3.11 is considered to have a constant percent opal. This core has the longest record of sediment with respect to length compared to the other cores. However, the 2000 cm of core only accounts for 30 000 years. Therefore there is high accumulation rate of sediment at the location of core MD98-2181 presumably due to its proximity to land.

Core TR163-22 was recovered from the EEP. The graph representing percent opal versus core depth is seen in Figure 3.12. The main feature is a major increase in percent opal that occurs between depths 380-500 cm. The average opal percent at its height is 35.0. Values are 23.0 % opal (0-360 cm) and 25.6% opal (520-880 cm) for the average of data points to either side of the high percent opal. One outlier occurs at 580 cm depth; the first result from this depth was 10.9 % opal after rerunning the sample the value came out to 34.5 %. The increase in opal seen at 800 cm depth is noted but since the duration of the increase is not sufficient it was left out of analysis.

Core ME 24 in figure 3.13 follows the same general pattern as core TR163-22 with one main difference (data points recorded between 0-522 cm is taken from Kienast et al. 2006). There are two significant increases in percent opal that occur at depths of 84.5 to 224.5 cm and another increase from 592-732 cm. Again there is evidence for an additional increase in percent opal between 1188 and1593 cm but frequency of sampling differs at this interval compared to the first increase seen in Figure 3.13. In the first increase from 84.5 to 224.5 cm samples are taken every one to three centimetres in contrast to the increase that occurred between 1188 and 1593 cm where samples were taken every twenty to thirty centimetres. During the first 522 cm of the core each sample represents 232 years but from 522 cm down each sample represents 2747 years. For this reason the apparent increase in percent opal from 1188 to 1593 cm is not described in this thesis. The increase in percent opal seen at 592 to 732 cm is accounted for due to the magnitude of the increase compared to the surrounding data points. On average, at that depth the percent opal was 38.6 a considerably increase as no other data points reach above a value of 30% opal (except for one).

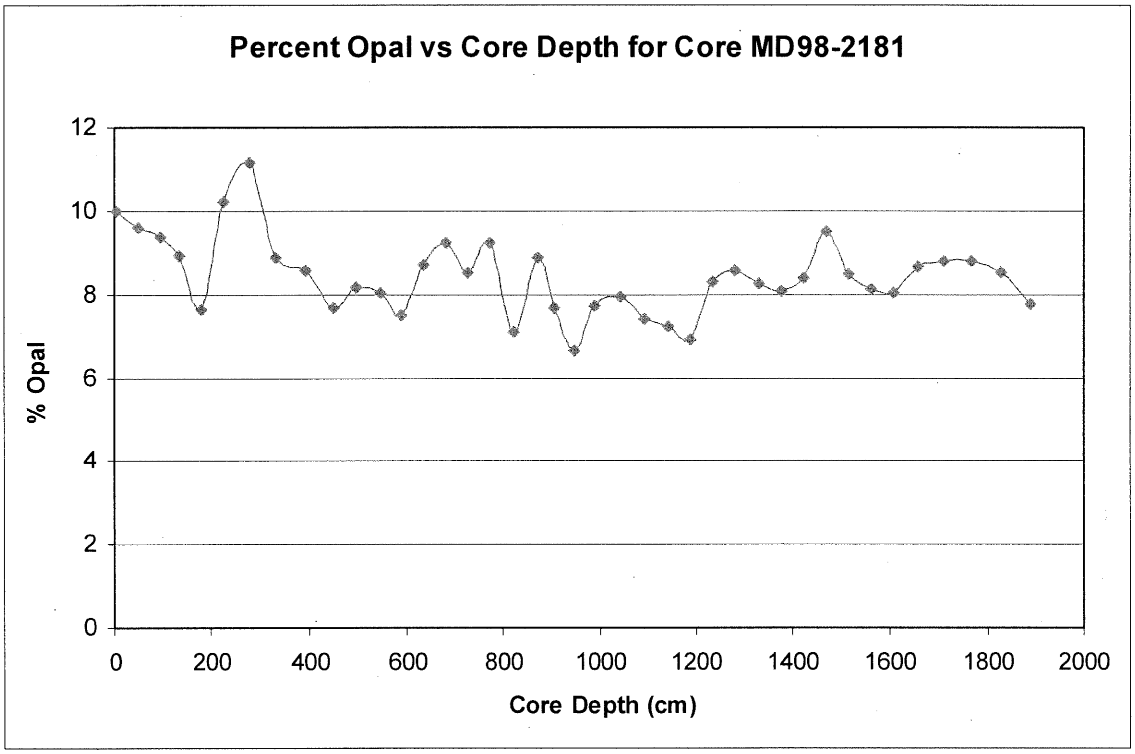

Figure 3.11 Percent opal versus core depth for Core MD98-2181

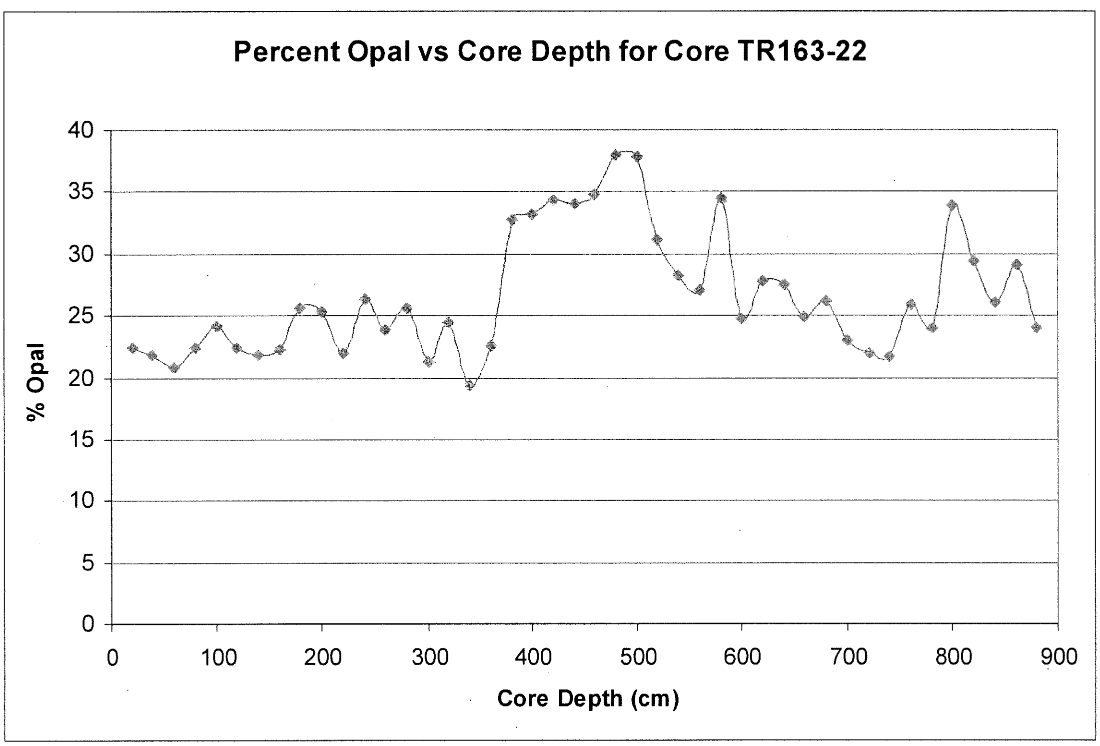

Figure 3.12 Percent opal versus core depth for Core TR163-22

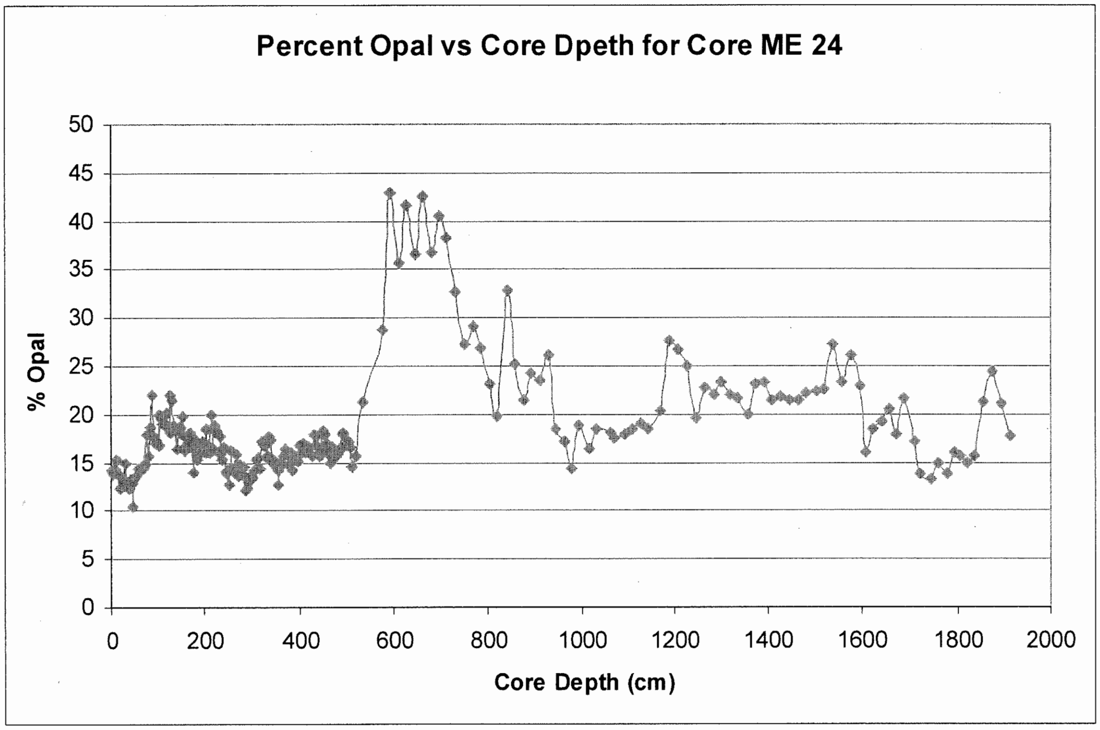

Figure 3.13 Percent opal versus core depth for Core ME 24

3.2 Percent Opal versus Age

Figure 3.20 shows the percent opal changes over time in each of the four cores. The ages of the cores are determined from oxygen isotope stratigraphy. The error for the ages given is ± 5000 years during glacial periods and ± 1000-2000 years during interglacial periods (M. Kienast pers. communication 2008). The percent opal values are lower in cores MD98-2181 and MD06-3067 which are found in the WEP. Most variability in the range of percent opal is found in cores ME 24 and TR163-22 indicative of the upwelling off Peru that transports silicic acid and other nutrients to the surface (Kienast et al. 2006). The most predominant increase in percent opal occurs around 50 ka in both the cores found in the EEP. Core ME 24 shows an increase in percent opal at approximately 20 ka but core TR163-22 and MD98-2181do not seem to mimic that pattern. However, the increase is seen in core MD06-3067 (more clearly seen in Figure 3.10) occurs at the same time as core ME 24 around 20 ka. This increase lasts much longer occurring over a 180 kyrs time span versus a 10 kyrs time period. In all likely hood the increase seen in core MD06-3067 is not associated with the Last Glacial Maximum since its beginning is some 20 000 years ago.

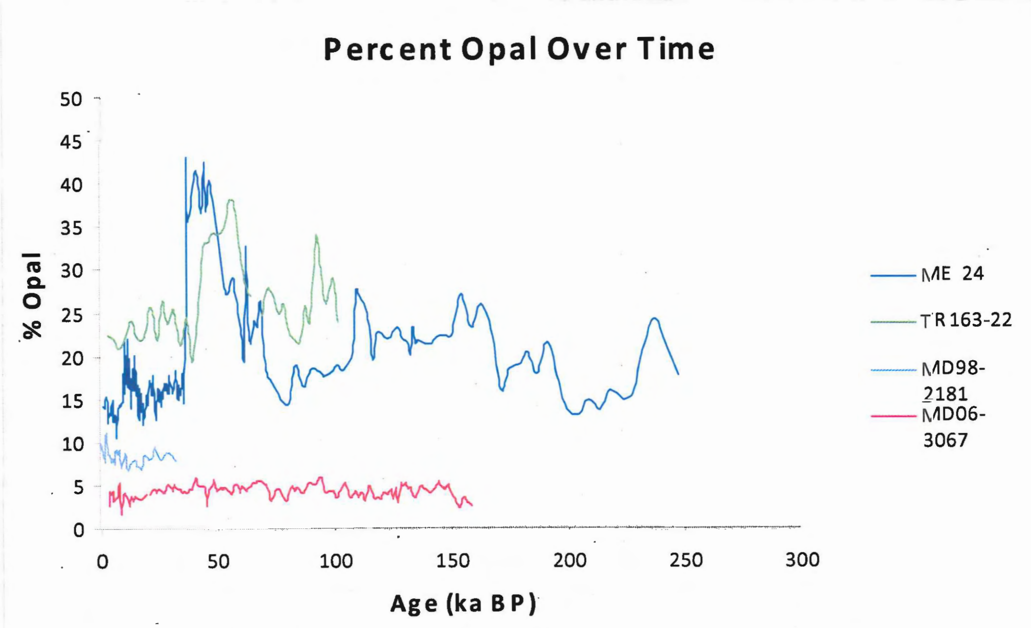

Figure 3.2 Includes all the cores in a comparison of percent opal over time.

4.0 DISCUSSION

4.1 Using percent opal as a paleoproxy

Two main problems arise when using percent opal as a paleoproxy for primary productivity by siliceous organisms. The first is dilution of the opal and the second is the dissolution and preservation of biogenic opal. The dilution problem is due to measuring biogenic opal as a percent. Marine sediment mainly comprises calcium carbonate, detrital sediment and biogenic opal. If one of these constituents fluctuates then the percent of each will change accordingly because all three components equal 100 percent. In an area that has a high rate of sedimentation coming from a terrestrial source the percent opal would be lower than in an area that was not experiencing increased sediment input. Cores in the open ocean would be less influenced by the input of terrestrial sediment while cores closer to land as in the case of core MD98-2181 would be more influenced.

The problem of dissolution and preservation is more complicated with many factors that need to be considered. Dissolution affects the amount of biogenic opal that reaches the ocean floor by going into solution and being recycled within the euphotic zone. On average 60% of biogenic silica produced in surface water goes into solution in the first 50 to 100 meters of the water column (Raguneau et al. 2000). That being said there are factors that contribute to the overall dissolution rate of biogenic opal. The equation for opal's dissolution rate is seen in equation 4.0 and taken from Ragueneau et al. paper 2000.

$$V_{dis} = k\ ([Si(OH)_4]_{sat} - [Si(OH)_4]\ A_{sp} \qquad (4.0)$$

Where:

V_{dis} is the dissolution rate of opal in seawater

k is the first order rate constant

$Si(OH)_{4sat}$ is the solubility of opal

$Si(OH)_4$ is the ambient silica acid concentration

A_{sp} is the surface area of opal present

Temperature affects both the rate constant and the solubility of biogenic opal. If temperatures are warmer then an increase occurs in both these factors leading to an increase in the dissolution rate. The silicic acid concentration has little effect on the dissolution rate unless the opal crystal structure contains trace elements such as aluminium in place of silicon. The surface area of opal takes into consideration that different diatom species have different dissolution rates (Ragueneau et al. 2000).

Other factors affect the solubility of opal as well. The biogenic opal is covered in organic material that must be stripped before dissolution of the opal can occur. This process occurs through microbial degradation or grazing. The best way for opal to avoid dissolution is through fecal pellets or flocculation. When grazers consume diatoms their opal structures are preserved and expelled through the grazer's fecal matter. Due to the weight and the protection fecal pellets provide, biogenic opal is delivered to the ocean floor faster and with limited contact to sea water. In the same fashion, flocculation works to minimize the solubility of biogenic opal in the under saturated surface waters by quickly transporting it to the deep ocean. The weight of the aggregate of opal accomplishes this. These factors all combine to lower the amount of recycling that occurs in the surface waters and increase the export of biogenic opal to be preserved in the sediment record.

4.2 Discussion of results

Figure 4.20 shows cores ME 24 and TR163-22 compared to the core results from Kienast et al. 2006 paper with respect to percent opal. The strongest correlation occurs between 40-60 ka BP. All cores in Figure 4.2 show an increase in percent opal during this time frame (except for ME 27 because the record does not go back that far). A problem arises when looking at the data from the Last Glacial Maximum (LGM) that occurred between 19-23 ka BP. Not all the cores show an increase in percent opal during the LGM. Cores ME 24, ME 27 and TR163-31 all show an increase in percent opal. This is considered an increase due to the strong correlation from the three cores; where as in other peaks only one core exhibits a rise in percent opal. Neither Kienast et al. 2006 nor Bradtmiller at al. 2006 record an increase during the LGM. There is no strong signal in the rise of percent opal for the glacial period that occurred 125-200 ka. Cores MD98-2181 and MD06-3067 located in the WEP are affected in terms of percent opal but to much lesser extent then cores from the EEP.

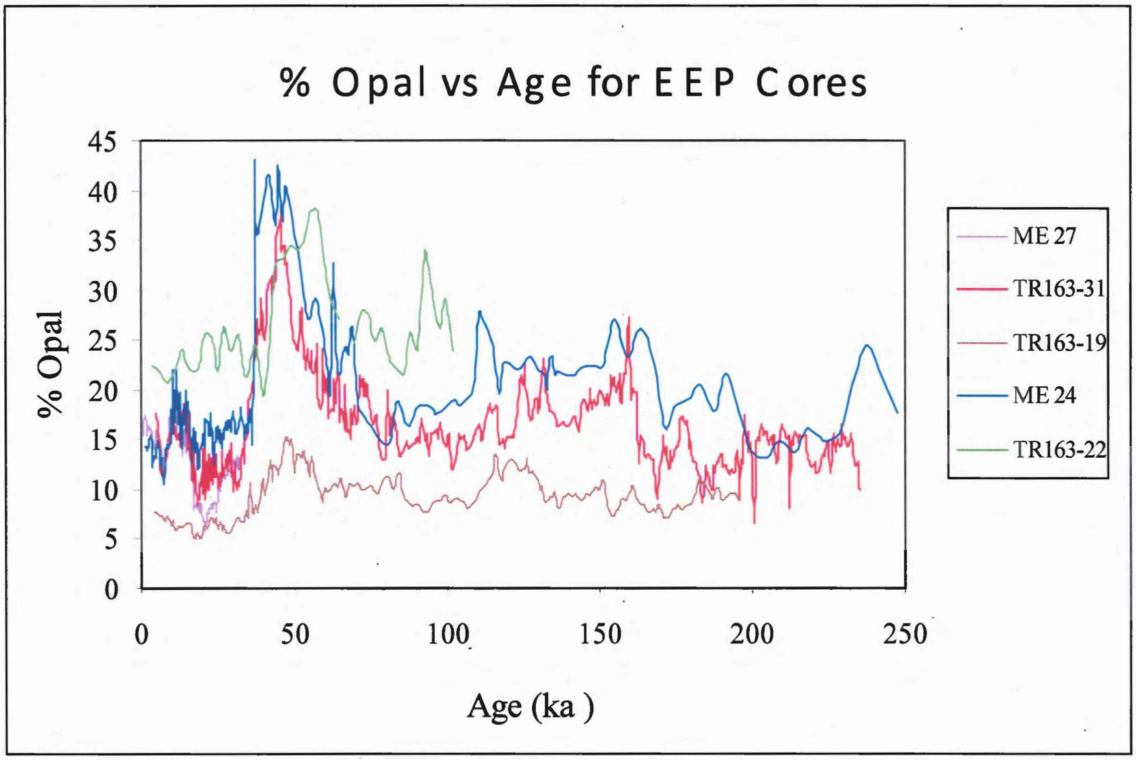

Figure 4.20 Compares the results from this thesis (cores ME 24 and TR163-22) and from the Kienast et al. 2006 paper (cores ME 27, TR163-31 and TR163-19). All cores are from the Eastern Equatorial Pacific.

Water travels via the South Equatorial Current (SEC) and North Equatorial Current (NEC) to the WEP before it reaches there it upwells from the Equatorial Undercurrent (EUC) off the coast of Peru in the EEP. A main contributor to the EUC is Subantarctic Mode Water which comes directly from the Southern Ocean (Kienast et al. 2006). Nutrients get used up before travelling to the WEP causing the productivity and therefore the biogenic opal to be reduced compared to the EEP. No peaks in percent opal were observed in either core of the WEP for any given period of glaciation.

Since the only cores to show an increase in percent opal were the two recovered from the EEP and only between the contribution of the silica leakage hypothesis to atmospheric CO_2

levels might be minimal. However, the strong signal seen at 40-60 kyrs BP in cores TR163-22 and ME 24 could reflect the possibility of the silica leakage hypothesis occurring when optimal conditions present themselves. Between 40-60 ka sea ice cover was high and the dust flux was low in the Southern Ocean (SO) (Kienast et al 2006). The extent of sea ice plus the flux in iron over the last 200 ka is better represented in Figure 4.21. Sea ice cover limits the productivity of diatom growth causing silica acid to build up in the SO (Takeda 1998).

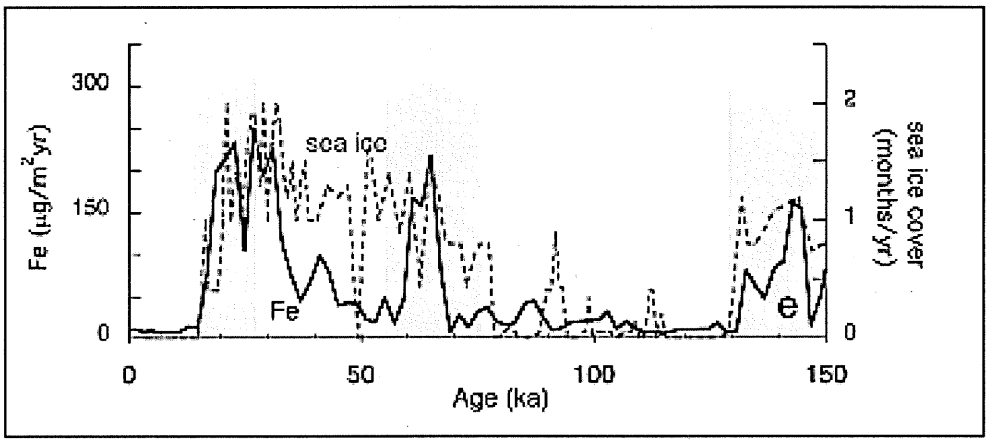

Figure 4.21 Shows the extent of sea ice in the Antarctic and the flux of iron in the Subantarctic for the last 150 000 years (Kienast et al. 2006).

5.0 Conclusion

The validity of the silica leakage hypothesis as a main component in the change of atmospheric CO_2 over glacial/interglacial time periods is debatable. While some cores show promising results with respect to peak percent opal values occurring at glacial times more then one problem arises. First of all not every period of glaciation appears in the sedimentary record with respect to an increase in percent opal. With that said, it is proposed that optimal conditions such as extensive sea ice cover and iron flux must be present in order to evoke the silica leakage hypothesis. Secondly, only the cores from the EEP show any strong signal at all that corresponds with a glacial period. Water that upwells off the coast of Peru and at the equator does reach cores found in the EEP first before circulating to the west; accounting for the low percent opal found in WEP cores compared to the EEP cores. Although the hypothesis does fit with the EEP cores between 40-60 ka, a different hypothesis for the lower CO_2 levels during glacial times needs to be called upon. There must be a different mechanism for the low levels of CO_2; the silica leakage plays a contributing role when conditions are optimal.

Works Cited

Bradtmiller, L.I., R.F. Anderson, M.Q. Fleisher and L.H. Burckle (2006), Diatom productivity in the equatorial Pacific Ocean from the last glacial period to the present: A test of the silicic acid leakage hypothesis, *Paleoceanography*, 21, PA4201, doi:10.1029/2006PA001282.

Broecker, Wallace S. The role of the ocean in climate yesterday, today and tomorrow. Eldigio Press: New York, 2004.

Brzezinski, M.A., C.J. Pride, V.M. Franck, D.M. Sigman, J.L. Sarmiento, K. Matsumoto, N. Gruber, G.H. Rau, K.H. Coale. (2002) A switch from Si(OH)4 to NO3- depletion in the glacial Southern Ocean. Geophysical Research Letters, 29(12) doi:10.1029/2001GL014349

Kienast, M. Personal Communication. February 5, 2008.

Kienast, S.S., M. Kienast, S. Jaccard, S.E. Calvert and R Francois (2006), Testing the silica leakage hypothesis with sedimentary opal records from eastern equatorial Pacific over the last 150 kyrs, *Geophysical Research Letters*, 33, L15607, doi:10.1029/2006GL026651.

Matsumoto, Katsumi, Jorge L. Sarmiento and Mark A. Brzezinski (2002), Silicic acid leakage from the Southern Ocean: A possible explanation for glacial atmospheric pCO_2, *Global Biogeochemical Cycles*, 16(3), 1031, doi:10/1029/2001GB001442.

Mortlock, R. and P.N. Froelich (1989) A simple method for the rapid determination of biogenic opal in pelagic marine sediments. Deep Sea Research 36, 1415-1426.

Petit, J. R., J. Jouzel, D. Raynaud, N.I. Barkov, J.M. Barnola, I. Basile, M. Benders, J. Chappellaz, M. Davis, G. Delaygue, M. Delmotte, V.M. Kotlyakov, M. Legrand, V.Y. Lipenkov, C. Lorius, L. Pepin, C. Ritz, E. Saltzman and M. Stievnard. (1999) Climate and atmospheric history of the past 420,000 years from the Vostok ice core, Antarctica. Nature 399, 429-436.

Sarmiento J.L., J. Simeon, A. Gnanadesikan, N. Gruber, R.M. Key and R. Schlitzer. (2007) Deep ocean biogeochemistry of silicic acid and nitrate. Global Biogeochemical Cycles, 21, GB1S90, doi:10.1029/2006GB002720.

Sarmiento, J.L., N, Gruber, M.A. Brzezinski and J.P. Dunne (2004), High-latitude controls of thermocline nutrients and low latitude biological productivity, *Nature,* 427, 56-60.

Sigman, Daniel M. and Edward A. Boyle (2000), Glacial/interglacial variations in atmospheric carbon dioxide, *Nature*, 407, 859-869.

Takeda, Shigenobu. (1998) Influence of iron availability on nutrient consumption ratio of diatoms in oceanic waters. Nature, 393, 774-777.

Treguer, Paul and Philippe Pondaven (2000), Silica control of carbon dioxide, *Nature*, 406, 358-359.

The International Research Institute for Climate and Society. (2007). Retrieved on January 7, 2008 http://iridl.ldeo.columbia.edu/SOURCES/.LEVITUS94/.ANNUAL/.

Appendix
Analytical Batch #1

Sample #	Weight (mg)	au	corrected au	Si mM	%Si (opal)	% opal	Depth (cm)	Age (ka)
67 I 12-13	19.75	0.0631	0.0419	0.393	1.117	2.680	12	3.997
67 I 20-21	20.83	0.0839	0.0627	0.587	1.584	3.802	20	4.184
67 I 30-31	21.22	0.0938	0.0726	0.680	1.801	4.322	30	4.434
67 I 40-41	19.64	0.0845	0.0633	0.593	1.696	4.071	40	4.711
67 I 50-51	19.79	0.0833	0.0621	0.582	1.652	3.964	50	5.038
67 I 60-61	20.01	0.0901	0.0689	0.646	1.812	4.350	60	5.409
67 I 70-71	22.18	0.0795	0.0583	0.546	1.383	3.320	70	5.875
67 I 90-91	21.35	0.0841	0.0629	0.589	1.551	3.722	90	7.092
67 I 100-101	19.86	0.0847	0.0635	0.595	1.683	4.039	100	7.802
67 I 110-111	19.19	0.1015	0.0803	0.752	2.202	5.286	110	8.544
67 I 120-121	21.42	0.0513	0.0301	0.282	0.740	1.775	120	9.309
67 I 130-131	20.61	0.0823	0.0611	0.573	1.560	3.745	130	10.104
67 I 140-141	18.56	0.0838	0.0626	0.587	1.775	4.261	140	10.911
67 II 0-1	22.07	0.0812	0.06	0.562	1.431	3.434	150	11.729
67 II 10-11	20.05	0.0627	0.0415	0.389	1.089	2.615	160	12.563
67 II 20-21	19.96	0.0819	0.0607	0.569	1.601	3.841	170	13.403
67 II 30-31	20.93	0.0762	0.055	0.515	1.383	3.319	180	14.249
67 II 40-41	18.5	0.0777	0.0565	0.529	1.607	3.858	190	15.104
67 II 60-61	22.1	0.0821	0.0609	0.571	1.450	3.481	210	16.824
67 II 70-71	20.16	0.0773	0.0561	0.526	1.465	3.515	220	17.690
67 II 90-91	20.86	0.0887	0.0675	0.632	1.703	4.088	240	19.432
67 II 100-101	20.36	0.1996	0.1784	1.672	4.612	11.068	250	20.307
67 II 110-111	20.74	0.0862	0.065	0.609	1.650	3.959	260	21.184
67 II 120-121	20.13	0.0928	0.0716	0.671	1.872	4.493	270	22.067
67 II 130-131	19.66	0.0925	0.0713	0.668	1.909	4.581	280	22.949
67 II 140-141	22.58	0.0978	0.0766	0.718	1.786	4.285	290	23.832
67 III 0-1	19.1	0.0907	0.0695	0.651	1.915	4.596	300	24.714
67 III 10-11	21.98	0.1026	0.0814	0.763	1.949	4.678	310	25.597
67 III 20-21	20.66	0.09	0.0688	0.645	1.753	4.207	320	26.480
67 III 30-31	20.22	0.0901	0.0689	0.646	1.793	4.304	330	27.361
67 III 40-41	19.82	0.0929	0.0717	0.672	1.904	4.570	340	28.244
67 III 50-51	21.03	0.1071	0.0859	0.805	2.150	5.160	350	29.127
67 III 60-61	21.95	0.1047	0.0835	0.782	2.002	4.805	360	30.010
67 III 70-71	21.45	0.0964	0.0752	0.705	1.845	4.429	370	30.892
67 III 80-81	19.66	0.1005	0.0793	0.743	2.123	5.095	380	31.775
67 III 90-91	20.44	0.0992	0.078	0.731	2.009	4.820	390	32.657
67 III 100-101	21.85	0.1002	0.079	0.740	1.903	4.567	400	33.540
67 III 110-111	19.85	0.0942	0.073	0.684	1.936	4.646	410	34.422
67 III 120-121	21.28	0.0932	0.072	0.675	1.781	4.274	420	35.305
67 III 130-131	19.76	0.0897	0.0685	0.642	1.825	4.379	430	36.188
67 III 140-141	20.67	0.0907	0.0695	0.651	1.770	4.247	440	37.071
67 IV 0-1	22.47	0.1024	0.0812	0.761	1.902	4.565	450	37.953
67 IV 10-11	20.26	0.0936	0.0724	0.678	1.881	4.514	460	38.835

Sample #	Weight (mg)	au	corrected au	Si mM	%Si (opal)	% opal	Depth (cm)	Age (ka)
67 IV 20-21	19.22	0.0911	0.0699	0.655	1.914	4.594	470	39.718
67 IV 30-31	21.12	0.121	0.0998	0.935	2.487	5.969	480	40.600
67 IV 40-41	19.06	0.1016	0.0804	0.753	2.220	5.328	490	41.483
67 IV 50-51	20.87	0.1038	0.0826	0.774	2.083	5.000	500	42.366
67 IV 80-81	21.2	0.1007	0.0795	0.745	1.974	4.737	530	45.013
67 IV 90-91	20.3	0.0656	0.0444	0.416	1.151	2.763	540	45.895
67 IV 100-101	22.77	0.105	0.0838	0.785	1.937	4.649	550	46.777
67 IV 110-111	20.47	0.1024	0.0812	0.761	2.088	5.011	560	47.652
67 IV 120-121	19.8	0.1116	0.0904	0.847	2.403	5.767	570	48.521
67 IV 130-131	20.83	0.1053	0.0841	0.788	2.125	5.100	580	49.388
67 IV 140-141	19.57	0.0906	0.0694	0.650	1.867	4.480	590	50.255
67 V 0-1	23.51	0.1113	0.0901	0.844	2.017	4.841	600	51.121
67 V 10-11	23.69	0.1098	0.0886	0.830	1.968	4.724	610	51.987
67 V 20-21	19.75	0.0929	0.0717	0.672	1.911	4.586	620	52.854
67 V 30-31	20.08	0.096	0.0748	0.701	1.961	4.706	630	53.720
67 V 50-51	20.66	0.0948	0.0736	0.690	1.875	4.500	640	54.587
67 V 60-61	20.74	0.0884	0.0672	0.630	1.705	4.093	660	56.320
67 V 70-71	21.1	0.1034	0.0822	0.770	2.050	4.921	670	57.186
67 V 80-81	19.38	0.0996	0.0784	0.735	2.129	5.110	680	58.053
67 V 90-91	22.38	0.1088	0.0876	0.821	2.060	4.944	690	58.919
67 V 100-101	18.96	0.0856	0.0644	0.603	1.788	4.291	700	59.786
67 V 110-111	20.14	0.1001	0.0789	0.739	2.062	4.949	710	60.652
67 V 120-121	20.28	0.0975	0.0763	0.715	1.980	4.753	720	61.535
67 V 130-131	20.69	0.0925	0.0713	0.668	1.814	4.353	730	62.477
67 V 140-141	19.55	0.0951	0.0739	0.692	1.990	4.775	740	63.499
67 VI 0-1	20.84	0.1035	0.0823	0.771	2.079	4.989	750	64.587
67 VI 10-11	21.7	0.1132	0.092	0.862	2.231	5.355	760	65.684
67 VI 20-21	19.44	0.1034	0.0822	0.770	2.226	5.341	770	66.781
67 VI 30-31	19.42	0.1064	0.0852	0.798	2.309	5.542	780	67.879
67 VI 40-41	18.42	0.1036	0.0824	0.772	2.354	5.651	790	68.976
67 VI 50-51	22.26	0.1118	0.0906	0.849	2.142	5.141	800	70.073
67 VI 60-61	19.59	0.1006	0.0794	0.744	2.133	5.120	810	71.171
SN Bulk	20.22	0.5073	0.4861	4.555	12.653	30.368		
JV Bulk	21.7	0.2257	0.2045	1.916	4.960	11.904		

Analytical Batch #2

Sample #	Weight mg	au	corrected au	Si mM	% Si (opal)	% opal	Core Dept	Age (ka)
67 I 120-121	20.86	0.0895	0.063	0.602	1.62	3.888	120	9.309
67 II 100-101	19.46	0.0964	0.0699	0.668	1.927	4.625	250	20.307
67 IV 90-91	23.83	0.0876	0.0611	0.584	1.375	3.301	540	45.895
67 I 90-91, 1	24.02	0.1053	0.0788	0.753	1.76	4.224	90	7.092
68 I 90-91, 2	20.12	0.0899	0.0634	0.605	1.69	4.057	90	7.092
69 I 90-91, 3	20.57	0.0895	0.063	0.602	1.643	3.943	90	7.092
67 V 90-91, 1	20.36	0.1024	0.0759	0.725	2	4.8	690	58.919
67 V 90-91, 2	19.23	0.103	0.0765	0.731	2.134	5.122	690	58.919
67 V 90-91, 3	21.54	0.1016	0.0751	0.717	1.87	4.489	690	58.919

Sample #	Weight (mg)	au	corrected au	Si mM	%Si (opal)	% opal	Depth (cm)	Age (ka)
67 VI 70-71	19.27	0.0842	0.0577	0.551	1.606	3.855	820	72.268
67 VI 80-81	23.06	0.0841	0.0576	0.55	1.34	3.216	830	73.366
67 VI 90-91	19.84	0.089	0.0625	0.597	1.69	4.056	840	74.463
67 VI 100-110	19.58	0.0952	0.0687	0.656	1.882	4.517	850	75.561
67 VI 110-111	22.76	0.1063	0.0798	0.762	1.881	4.514	860	76.658
67 VI 120-121	20.18	0.0911	0.0646	0.617	1.717	4.121	870	77.756
67 VI 130-131	19.24	0.0776	0.0511	0.488	1.425	3.419	880	78.853
67 VI 140-141	19.52	0.0796	0.0531	0.507	1.459	3.502	890	79.950
67 VII 0-1	19.77	0.0939	0.0674	0.644	1.829	4.389	900	81.048
67 VII 10-11	21.29	0.1087	0.0822	0.785	2.071	4.971	910	82.145
67 VII 20-21	22.67	0.1045	0.078	0.745	1.846	4.43	920	83.251
67 VII 30-31	20.61	0.1027	0.0762	0.728	1.983	4.76	930	84.402
67 VII 40-41	18.11	0.0867	0.0602	0.575	1.783	4.28	940	85.703
67 VII 50-51	20.27	0.0936	0.0671	0.641	1.776	4.262	950	87.223
67 VII 60-61	22.27	0.115	0.0885	0.845	2.132	5.116	960	88.823
67 VII 70-71	20.58	0.1131	0.0866	0.827	2.257	5.418	970	90.423
67 VII 80-81	21.22	0.1108	0.0843	0.805	2.131	5.115	980	92.023
67 VII 90-91	22.18	0.1293	0.1028	0.982	2.486	5.967	990	93.623
67 VII 100-101	18.41	0.1107	0.0842	0.804	2.453	5.888	1000	95.220
67 VII 110-111	20.26	0.0923	0.0658	0.628	1.742	4.181	1010	96.817
67 VII 120-121	20.37	0.0963	0.0698	0.667	1.838	4.412	1020	98.417
67 VII 130-131	24.2	0.1091	0.0826	0.789	1.831	4.394	1030	100.014
67 VII 140-141	21.92	0.0889	0.0624	0.596	1.527	3.665	1040	101.615
67 VIII 0-1	23.46	0.1122	0.0857	0.818	1.96	4.703	1050	103.220
67 VIII 10-11	21.9	0.1176	0.0911	0.87	2.232	5.356	1060	104.818
67 VIII 20-21	19.97	0.0879	0.0614	0.586	1.649	3.958	1070	106.414
67 VIII 30-31	21.98	0.0885	0.062	0.592	1.513	3.632	1080	107.909
67 VIII 40-41	20.8	0.0987	0.0722	0.69	1.862	4.469	1090	109.229
67 VIII 50-51	24.41	0.0972	0.0707	0.675	1.554	3.729	1100	110.378
67 VIII 60-61	19.04	0.0878	0.0613	0.585	1.727	4.145	1110	111.463
67 VIII 70-71	22.2	0.0967	0.0702	0.67	1.696	4.071	1120	112.543
67 VIII 80-81	22.44	0.0842	0.0577	0.551	1.379	3.31	1130	113.617
67 VIII 90-91	18.78	0.095	0.0685	0.654	1.957	4.696	1140	114.695
67 VIII 100-101	19.85	0.102	0.0755	0.721	2.04	4.897	1150	115.776
67 VIII 110-111	21.97	0.0878	0.0613	0.585	1.497	3.592	1160	116.849
67 VIII 120-121	21.59	0.0834	0.0569	0.543	1.414	3.393	1170	117.927
67 VIII 130-131	20.32	0.0826	0.0561	0.536	1.481	3.554	1180	119.008
67 VIII 140-141	20.44	0.0806	0.0541	0.517	1.42	3.408	1190	120.089
67 IX 0-1	19.89	0.0919	0.0654	0.625	1.764	4.233	1200	121.170
67 IX 10-11	21.99	0.096	0.0695	0.664	1.695	4.069	1210	122.246
67 IX 20-21	21.68	0.0951	0.0686	0.655	1.697	4.074	1220	123.319
67 IX 30-31	21.28	0.1017	0.0752	0.718	1.896	4.55	1230	124.396
67 IX 40-41	24.64	0.0929	0.0664	0.634	1.446	3.469	1240	125.476
67 IX 50-51	21.38	0.106	0.0795	0.759	1.995	4.787	1250	126.556
67 IX 60-61	19.67	0.0732	0.0467	0.446	1.274	3.057	1260	127.636
67 IX 70-71	22.63	0.1212	0.0947	0.904	2.245	5.388	1270	128.709

Sample #	Weight (mg)	au	corrected au	Si mM	%Si (opal)	% opal	Depth (cm)	Age (ka)
67 IX 80-81	20.07	0.1045	0.078	0.745	2.085	5.004	1280	129.786
67 IX 90-91	18.57	0.1033	0.0768	0.733	2.219	5.325	1290	130.866
67 IX 100-101	18.54	0.0926	0.0661	0.631	1.913	4.59	1300	131.946
67 IX 110-111	20.28	0.1027	0.0762	0.728	2.016	4.838	1310	133.019
67 IX 120-121	18.75	0.0827	0.0562	0.537	1.608	3.859	1320	134.096
67 IX 130-131	21.82	0.089	0.0625	0.597	1.537	3.688	1330	135.176
67 IX 140-141	20.73	0.0944	0.0679	0.648	1.757	4.217	1340	136.254
67 X 0-1	19.43	0.1022	0.0757	0.723	2.09	5.016	1350	137.330
67 X 10-11	19.39	0.095	0.0685	0.654	1.895	4.548	1360	138.406
67 X 20-21	22.37	0.1058	0.0793	0.757	1.902	4.564	1370	139.486
67 X 30-31	23.46	0.1037	0.0772	0.737	1.765	4.237	1380	140.566
67 X 40-41	24.25	0.1058	0.0793	0.757	1.754	4.21	1390	141.639
67 X 50-51	23.3	0.1109	0.0844	0.806	1.943	4.664	1400	142.716
67 X 60-61	20.14	0.101	0.0745	0.711	1.984	4.762	1410	143.796
67 X 70-71	18.05	0.1046	0.0781	0.746	2.321	5.571	1420	144.876
67 X 80-81	23.06	0.115	0.0885	0.845	2.059	4.941	1430	145.956
67 X 90-91	21.43	0.1067	0.0802	0.766	2.008	4.818	1440	147.029
67 X 100-101	20.38	0.1001	0.0736	0.703	1.937	4.65	1450	148.106
67 X 110-111	18.88	0.1024	0.0759	0.725	2.157	5.176	1460	149.186
67 X 120-121	21.5	0.0997	0.0732	0.699	1.826	4.383	1470	150.266
67 X 130-131	19.63	0.0806	0.0541	0.517	1.478	3.548	1480	151.339
67 X 140-141	23.09	0.0894	0.0629	0.601	1.461	3.507	1490	152.418
67 XI 0-1	20.37	0.0674	0.0409	0.391	1.077	2.585	1500	153.500
67 XI 10-11	24.14	0.0718	0.0453	0.433	1.007	2.416	1510	154.576
67 XI 20-21	23.22	0.0928	0.0663	0.633	1.532	3.676	1520	155.649
67 XI 30-31	24.62	0.0865	0.06	0.573	1.307	3.138	1530	156.726
67 XI 40-41	21.37	0.0778	0.0513	0.49	1.288	3.091	1540	157.806
67 XI 50-51	23.26	0.0757	0.0492	0.47	1.135	2.723	1550	158.886
SN Bulk	21.66	0.5715	0.545	5.205	13.498	32.395		
JV Bulk	21.64	0.2125	0.186	1.776	4.611	11.066		

Analytical Batch #3

Sample #	Weight mg	au	corrected au	Si mM	%Si (opal)	% opal	Depth (cm)	Age (ka)
TR 20	20.3	0.3991	0.3576	3.379	9.351	22.442	20	3.533
TR 40	20.78	0.3972	0.3557	3.361	9.086	21.807	40	6.156
TR 60	21.39	0.3906	0.3491	3.299	8.663	20.792	60	8.749
TR 80	19.62	0.3875	0.346	3.270	9.361	22.467	80	11.336
TR 100	20.64	0.4323	0.3908	3.693	10.051	24.122	100	13.466
TR 120	21.78	0.4249	0.3834	3.623	9.344	22.426	120	15.222
TR 140	21.68	0.4127	0.3712	3.508	9.089	21.813	140	16.988
TR 160	19.68	0.386	0.3445	3.256	9.292	22.301	160	18.950
TR 180	18.25	0.4082	0.3667	3.465	10.666	25.598	180	20.912
TR 200	19.46	0.4275	0.386	3.648	10.529	25.270	200	22.867
TR 220	20.35	0.3912	0.3497	3.305	9.122	21.892	220	24.815
TR 240	22.48	0.5073	0.4658	4.402	10.999	26.398	240	26.763
TR 260	19.37	0.4039	0.3624	3.425	9.931	23.835	260	29.106

Sample #	Weight (mg)	au	corrected au	Si mM	%Si (opal)	% opal	Depth (cm)	Age (ka)
TR 280	19.36	0.43	0.3885	3.671	10.652	25.565	280	31.772
TR 300	22.15	0.4112	0.3697	3.494	8.860	21.264	300	34.438
TR 320	21.49	0.4536	0.4121	3.894	10.179	24.430	320	37.086
TR 340	20.67	0.3559	0.3144	2.971	8.074	19.378	340	39.403
TR 360	20.07	0.3966	0.3551	3.356	9.392	22.541	360	41.721
TR 380	19.46	0.5406	0.4991	4.716	13.614	32.674	380	44.038
TR 400	19.42	0.5475	0.506	4.782	13.831	33.194	400	46.356
TR 420	20.06	0.5826	0.5411	5.113	14.319	34.364	420	48.673
TR 440	20.44	0.5884	0.5469	5.168	14.203	34.087	440	50.991
TR 460	19.76	0.581	0.5395	5.098	14.493	34.783	460	53.308
TR 480	20.65	0.658	0.6165	5.826	15.848	38.034	480	55.626
TR 500	21.37	0.6766	0.6351	6.002	15.776	37.862	500	57.943
TR 520	20.85	0.552	0.5105	4.824	12.997	31.193	520	60.261
TR 540	22.51	0.5394	0.4979	4.705	11.741	28.179	540	62.578
TR 560	22.5	0.5191	0.4776	4.513	11.268	27.042	560	64.896
TR 580	21.37	0.2246	0.1831	1.730	4.548	10.916	580	67.213
TR 600	21.75	0.4629	0.4214	3.982	10.285	24.683	600	69.531
TR 622	22.36	0.53	0.4885	4.616	11.597	27.833	620	71.848
TR 640	23.06	0.5382	0.4967	4.694	11.434	27.441	640	74.166
TR 660	23.06	0.4915	0.45	4.253	10.359	24.861	660	76.483
TR 680	21.27	0.4776	0.4361	4.121	10.884	26.121	680	78.801
TR 700	21.27	0.4251	0.3836	3.625	9.573	22.976	700	81.118
TR 720	22.53	0.4301	0.3886	3.672	9.156	21.974	720	83.436
TR 740	22.03	0.4172	0.3757	3.550	9.053	21.726	740	85.753
TR 760	20.21	0.4513	0.4098	3.873	10.764	25.833	760	88.071
TR 780	21.57	0.4481	0.4066	3.842	10.006	24.015	780	90.388
TR 800	22.15	0.6295	0.588	5.557	14.091	33.819	800	92.706
TR 820	22.15	0.553	0.5115	4.834	12.258	29.419	820	95.023
TR 841	22.47	0.5016	0.4601	4.348	10.869	26.086	840	97.341
TR 860	22.81	0.5635	0.522	4.933	12.148	29.155	860	99.658
TR 880	24.05	0.4945	0.453	4.281	9.998	23.996	880	101.976
MD98-2181, 4	22.49	0.2182	0.1767	1.670	4.171	10.009	4	0.041
50	21.92	0.2064	0.1649	1.558	3.993	9.584	50	0.518
94	20.85	0.1949	0.1534	1.450	3.905	9.373	94	0.974
133	19.73	0.1794	0.1379	1.303	3.710	8.904	133	1.378
179	22.17	0.1744	0.1329	1.256	3.182	7.637	179	1.855
226	21.94	0.2176	0.1761	1.664	4.261	10.226	226	2.342
278	20.47	0.0073	-0.0342	-0.323	-0.887	-2.128	278	2.881
333	21.8	0.1932	0.1517	1.434	3.694	8.865	333	3.450
393	22.89	0.1952	0.1537	1.452	3.564	8.554	393	4.072
452	19.96	0.1614	0.1199	1.133	3.189	7.653	452	4.683
498	21.39	0.1785	0.137	1.295	3.400	8.160	498	5.160
545	22.1	0.1809	0.1394	1.317	3.348	8.036	545	5.647
590	21.84	0.17	0.1285	1.214	3.123	7.496	590	6.113
635	22.42	0.1947	0.1532	1.448	3.627	8.705	635	6.580

Sample #	Weight (mg)	au	corrected au	Si mM	%Si (opal)	% opal	Depth (cm)	Age (ka)
680	21.06	0.1939	0.1524	1.440	3.841	9.219	680	7.046
725	20.88	0.1815	0.14	1.323	3.559	8.542	725	7.688
771	20.54	0.1904	0.1489	1.407	3.848	9.235	771	8.372
823	21.77	0.1624	0.1209	1.143	2.948	7.075	823	9.355
871	20.38	0.1837	0.1422	1.344	3.704	8.889	871	10.489
905	22.18	0.175	0.1335	1.262	3.195	7.668	905	11.288
947	20.39	0.1479	0.1064	1.005	2.770	6.648	947	12.251
989	23.62	0.1844	0.1429	1.350	3.211	7.708	989	13.215
1045	24.09	0.0829	0.0414	0.391	0.912	2.189	1045	14.499
1095	21.42	0.1661	0.1246	1.177	3.088	7.411	1095	15.617
1142	20.32	0.157	0.1155	1.091	3.017	7.241	1142	16.543
1189	22.6	0.1639	0.1224	1.157	2.875	6.900	1189	17.468
1236	19.76	0.1704	0.1289	1.218	3.463	8.311	1236	18.375
1282	22.1	0.1901	0.1486	1.404	3.569	8.566	1282	19.263
1330	20.18	0.1722	0.1307	1.235	3.438	8.251	1330	20.222
1376	22.97	0.1869	0.1454	1.374	3.360	8.064	1376	21.144
1423	21.07	0.1805	0.139	1.314	3.502	8.405	1423	22.301
1469	20.21	0.1922	0.1507	1.424	3.958	9.500	1469	23.490
1514	20.97	0.1813	0.1398	1.321	3.539	8.493	1514	24.503
1561	21.06	0.1755	0.134	1.266	3.378	8.106	1561	25.465
1606	18.64	0.159	0.1175	1.110	3.346	8.031	1606	26.386
1654	22.61	0.1953	0.1538	1.453	3.611	8.666	1654	27.369
1710	22.97	0.2	0.1585	1.498	3.663	8.791	1710	28.515
1766	20.42	0.1823	0.1408	1.331	3.660	8.784	1766	29.661
1828	23.11	0.1957	0.1542	1.457	3.542	8.501	1828	30.930
1888	22.2	0.177	0.1355	1.280	3.240	7.776	1888	32.158
JV Bulk	23.57	0.2678	0.2263	2.139	5.097	12.232		
SN Bulk	22.41	0.6387	0.5972	5.644	14.146	33.950		
67 I 90-91	22.1	0.1077	0.0662	0.626	1.590	3.816	90	7.092
67 V 90-91	20	0.1143	0.0728	0.688	1.932	4.637	690	58.919

Analytical Batch #4

Sample #	Weight mg	au	corrected au	Si mM	%Si (opal)	% opal	Depth (cm	Age (ka)
ME-24, 500	22.87	0.3813	0.3457	3.177	7.803	18.728	500	36.107
516	23.06	0.3931	0.3575	3.285	8.003	19.207	516	36.250
536	21.01	0.3964	0.3608	3.316	8.865	21.276	536	36.471
576	24.13	0.5941	0.5585	5.133	11.948	28.676	576	37.117
592	19.29	0.7045	0.6689	6.147	17.900	42.961	592	37.450
612	20.55	0.6265	0.5909	5.430	14.844	35.625	612	37.950
628	19.4	0.6864	0.6508	5.981	17.317	41.562	628	41.238
648	21.26	0.663	0.6274	5.766	15.234	36.562	648	43.613
660	21.96	0.7894	0.7538	6.927	17.720	42.528	660	44.760
680	22.06	0.6911	0.6555	6.024	15.339	36.814	680	46.100
696	21.63	0.7408	0.7052	6.481	16.830	40.393	696	47.038
712	22.47	0.7291	0.6935	6.373	15.932	38.238	712	48.637
732	21.62	0.6043	0.5687	5.226	13.579	32.589	732	51.719

Sample #	Weight (mg)	au	corrected au	Si mM	%Si (opal)	% opal	Depth (cm)	Age (ka)
748	22.01	0.5187	0.4831	4.440	11.331	27.193	748	54.000
768	23.58	0.5896	0.554	5.091	12.128	29.108	768	56.800
784	22.01	0.5132	0.4776	4.389	11.202	26.884	784	58.567
804	22.42	0.4557	0.4201	3.861	9.673	23.215	804	60.567
820	24.51	0.4251	0.3895	3.580	8.204	19.688	820	61.633
840	20.96	0.5896	0.554	5.091	13.644	32.747	840	62.873
856	23.32	0.5106	0.475	4.365	10.515	25.235	856	63.663
876	20.76	0.396	0.3604	3.312	8.962	21.508	876	64.700
892	23.42	0.4933	0.4577	4.206	10.089	24.213	892	66.184
912	21.25	0.4379	0.4023	3.697	9.773	23.455	912	67.500
928	23.46	0.5319	0.4963	4.561	10.921	26.210	928	68.786
944	22.7	0.3728	0.3372	3.099	7.668	18.404	944	70.800
964	23	0.3542	0.3186	2.928	7.151	17.162	964	73.393
980	22.97	0.3033	0.2677	2.460	6.016	14.439	980	80.583
996	22.8	0.3832	0.3476	3.194	7.870	18.888	996	83.671
1016	23.09	0.3425	0.3069	2.820	6.861	16.467	1016	87.050
1032	20.37	0.3404	0.3048	2.801	7.724	18.538	1032	90.743
1062	21.32	0.346	0.3104	2.853	7.516	18.038	1062	94.893
1072	20.26	0.3233	0.2877	2.644	7.331	17.593	1072	95.979
1092	21.56	0.3478	0.3122	2.869	7.475	17.940	1092	98.308
1108	22.57	0.372	0.3364	3.092	7.694	18.466	1108	100.046
1128	20.23	0.345	0.3094	2.843	7.895	18.948	1128	102.416
1144	21.02	0.3478	0.3122	2.869	7.667	18.401	1144	104.429
1172	23.01	0.4148	0.3792	3.485	8.507	20.417	1172	108.371
1188	20.59	0.4945	0.4589	4.217	11.505	27.613	1188	110.137
1208	21.5	0.4983	0.4627	4.252	11.110	26.663	1208	112.091
1228	21.52	0.4684	0.4328	3.977	10.382	24.917	1228	114.438
1248	19.96	0.3501	0.3145	2.890	8.134	19.521	1248	117.217
1264	24.75	0.4917	0.4561	4.192	9.513	22.831	1264	118.900
1284	22.35	0.4314	0.3958	3.637	9.142	21.940	1284	123.344
1300	23.11	0.4717	0.4361	4.008	9.741	23.379	1300	127.135
1320	21.47	0.4181	0.3825	3.515	9.197	22.072	1320	129.760
1336	20.89	0.4013	0.3657	3.361	9.037	21.689	1336	131.800
1356	20.93	0.3743	0.3387	3.113	8.354	20.049	1356	133.077
1372	20.85	0.4245	0.3889	3.574	9.629	23.109	1372	133.781
1392	21.33	0.4367	0.4011	3.686	9.707	23.297	1392	134.734
1408	21.84	0.4153	0.3797	3.489	8.975	21.539	1408	135.543
1428	22.29	0.4284	0.3928	3.610	9.097	21.833	1428	136.889
1444	21.86	0.415	0.3794	3.487	8.959	21.503	1444	139.123
1464	22.01	0.4155	0.3799	3.491	8.910	21.384	1464	141.912
1480	21.56	0.4207	0.3851	3.539	9.221	22.129	1480	144.135
1504	23.19	0.4551	0.4195	3.855	9.338	22.412	1504	147.933
1519	21.48	0.4256	0.39	3.584	9.373	22.495	1519	150.916
1536	24.61	0.5754	0.5398	4.961	11.323	27.175	1536	155.000
1556	21.99	0.4491	0.4135	3.800	9.707	23.297	1556	159.333
1576	21.82	0.4951	0.4595	4.223	10.871	26.090	1576	163.500

Sample #	Weight (mg)	au	corrected au	Si mM	%Si (opal)	% opal	Depth (cm)	Age (ka)
1593	21.01	0.4244	0.3888	3.573	9.553	22.927	1593	167.750
1608	23.23	0.3377	0.3021	2.776	6.713	16.112	1608	171.500
1623	20.96	0.3488	0.3132	2.878	7.714	18.513	1623	175.250
1642	23.43	0.3992	0.3636	3.341	8.011	19.226	1642	180.000
1654	22.25	0.4034	0.3678	3.380	8.533	20.480	1654	183.000
1672	21.25	0.344	0.3084	2.834	7.492	17.981	1672	187.500
1688	21.92	0.4201	0.3845	3.534	9.055	21.732	1688	191.500
1708	20.52	0.319	0.2834	2.604	7.129	17.111	1708	196.500
1722	21.61	0.2749	0.2393	2.199	5.716	13.719	1722	200.000
1742	21.28	0.2623	0.2267	2.083	5.499	13.199	1742	205.000
1758	21.53	0.2957	0.2601	2.390	6.236	14.967	1758	209.000
1778	23.4	0.2946	0.259	2.380	5.714	13.713	1778	214.000
1792	19.95	0.2931	0.2575	2.366	6.663	15.991	1792	217.500
1806	23.36	0.3316	0.296	2.720	6.541	15.699	1806	221.000
1819	22.22	0.3034	0.2678	2.461	6.222	14.932	1819	224.250
1836	19.49	0.2817	0.2461	2.262	6.518	15.644	1836	228.500
1855	20.8	0.3921	0.3565	3.276	8.848	21.235	1855	233.250
1873	19.98	0.4289	0.3933	3.614	10.162	24.388	1873	237.750
1893	22.99	0.4268	0.3912	3.595	8.784	21.082	1893	242.750
1913	22.12	0.3526	0.317	2.913	7.398	17.755	1913	247.750
JV Bulk	20.33	0.2694	0.2338	2.149	5.937	14.248		
67 I 90-91	22.14	0.1522	0.1166	1.072	2.719	6.525	90	7.092
67 V 90-91	19.46	0.1572	0.1216	1.118	3.226	7.742	690	58.919
TR 580	22.66	0.6665	0.6309	5.798	14.373	34.494	710	67.213
MD98 278	21.52	0.2296	0.194	1.783	4.654	11.169	278	2.881
MD98 1045	19.98	0.1639	0.1283	1.179	3.315	7.956	1045	14.499